Pharm Res (2013) 30:104–116
DOI 10.1007/s11095-012-0853-y

RESEARCH PAPER

The Effect of Metal-Chelating Polymers (MCPs) for ^{111}In Complexed *via* the Streptavidin-Biotin System to Trastuzumab Fab Fragments on Tumor and Normal Tissue Distribution in Mice

Amanda J. Boyle • Peng Liu • Yijie Lu • Dirk Weinrich • Deborah A. Scollard • Ghislaine Ngo Njock Mbong • Mitchell A. Winnik • Raymond M. Reilly

Received: 16 April 2012 / Accepted: 2 August 2012 / Published online: 21 August 2012

ABSTRACT

Purpose To study the effects of backbone composition and charge of biotin-functionalized metal-chelating polymers (Bi-MCPs) for ^{111}In complexed to streptavidin (SAv)-trastuzumab Fab fragments on tumor and normal tissue localization.

Methods Bi-MCPs were synthesized with a polyacrylamide [Bi-PAm(DTPA)$_{40}$], polyaspartamide [Bi-PAsp(DTPA)$_{33}$] or polyglutamide [Bi-PGlu(DTPA)$_{28}$] backbone and harboured diethylenetriaminepentaacetic acid (DTPA) chelators for ^{111}In. Bi-PAm(DTPA)$_{40}$ had a net negative charge; Bi-PAsp(DTPA)$_{33}$ and Bi-PGlu(DTPA)$_{28}$ were zwitterionic with a net neutral charge. Binding to HER2+ SKOV-3 human ovarian carcinoma cells was determined. Tissue uptake was studied in Balb/c mice by MicroSPECT/CT imaging and biodistribution studies. Tumor and normal tissue uptake of ^{111}In-labeled Bi-PAsp(DTPA)$_{33}$ or Bi-PGlu(DTPA)$_{28}$ complexed to SAv-Fab was evaluated 48 h post-injection in athymic mice with subcutaneous SKOV-3 xenografts.

Results SAv-Fab complexed to MCPs bound specifically to SKOV-3 cells; but specific binding was decreased 2-fold. Liver uptake was 5–13 fold higher for Bi-PAm(DTPA)$_{40}$ than Bi-PAsp(DTPA)$_{33}$ and Bi-PGlu(DTPA)$_{28}$ but was reduced by decreasing negative charges by saturation with indium. ^{111}In-Bi-PAsp(DTPA)$_{33}$ complexed to SAv-Fab accumulated in SKOV-3 tumors; low tumor uptake was found for ^{111}In-Bi-PGlu(DTPA)$_{28}$-SAv-Fab.

Conclusions Zwitterionic MCPs composed of polyaspartamide with a net neutral charge are most desirable for constructing radioimmunoconjugates.

KEY WORDS HER2 immunoreactivity · indium-111 · metal-chelating polymers (MCPs) · trastuzumab · tumor and normal tissue distribution

ABBREVIATIONS

% ID/g	percent injected dose/gram
Bi	biotin
Bi-PAm(DTPA)$_{40}$	biotinylated polyacrylamide polymer with 40 pendant DTPA groups
Bi-PAsp(DTPA)$_{33}$	biotinylated polyaspartamide polymer with 33 pendant DTPA groups
Bi-PGlu(DTPA)$_{28}$	biotinylated polyglutamide polymer with 28 pendant DTPA groups
DMTMM	4-(4,6-dimethoxy-1,3,5-triazin-2-yl)-4-methylmorpholinium chloride
DP$_n$	Number average degree of polymerization
DTPA	diethylenetriaminepentaacetic acid
HER2	human epidermal growth factor receptor-2

A. J. Boyle · D. A. Scollard · G. Ngo Njock Mbong · R. M. Reilly
Department of Pharmaceutical Sciences, University of Toronto
Toronto, Ontario M5S 3M2, Canada

P. Liu · Y. Lu · D. Weinrich · M. A. Winnik (✉)
Department of Chemistry, University of Toronto
80 St. George St., Toronto, Ontario M5S 3H6, Canada
e-mail: mwinnik@chem.utoronto.ca

R. M. Reilly (✉)
Leslie Dan Faculty of Pharmacy, University of Toronto
144 College St., Toronto, Ontario M5S 3M2, Canada
e-mail: raymond.reilly@utoronto.ca

R. M. Reilly
Toronto General Research Institute, University Health Network
Toronto, Ontario M5G 2C4, Canada

R. M. Reilly
Department of Medical Imaging, University of Toronto
150 College St., Toronto, Ontario M5S 3E2, Canada

ITLC-SG	instant thin layer-silica gel chromatography
LE	labeling efficiency
MCP	metal-chelating polymer
NLS	nuclear translocation sequence
PAMAM	polyamidoamine
PAsp(DET)	polyaspartamide with diethylenetriamine pendant groups
PDI	polydispersity index
PGlu(DET)	polyglutamide with diethylenetriamine pendant groups
RAFT	reversible addition-fragmentation chain transfer
SA	specific activity
SAv	streptavidin
SM-PEG_{24}-NHS	succinimidyl-[(*N*-maleimidopropionamido)(1)-24-ethyleneglycol] ester

INTRODUCTION

The human epidermal growth factor receptor-2 (HER2) is overexpressed in 20–25% of cases of breast cancer and is the target for the immunotherapeutic agent, trastuzumab (Herceptin) (1). We have been investigating Auger electron radioimmunotherapy of HER2-positive tumors using trastuzumab modified with nuclear translocation sequence (NLS) peptides and derivatized with diethylenetriaminepentaacetic acid (DTPA) for labeling with ^{111}In (2). Release of nanometer-micrometer range Auger electrons in close proximity to the cell nucleus causes lethal DNA double-strand breaks. ^{111}In-NLS-trastuzumab was bound, internalized and transported to the nucleus of HER2-positive breast cancer cells likely due to interaction of the appended NLS peptides with importins α/β (3). ^{111}In-NLS-trastuzumab was 8-fold more potent than trastuzumab at decreasing the clonogenic survival of HER2-amplified SKBR-3 human breast cancer cells (2). Moreover, ^{111}In-NLS-trastuzumab killed trastuzumab-resistant tumor cells (4). Nonetheless, the potency of ^{111}In-NLS-trastuzumab was dependent on HER2 density. Increasing the amount of ^{111}In delivered per HER2 recognition event would enhance the potency of ^{111}In-NLS-trastuzumab for killing HER2-overexpressing tumor cells and potentially extend its effects to cells with moderate HER2 density. This can be appreciated by the fact that at the specific activity (SA) achieved for ^{111}In-NLS-trastuzumab monosubstituted with DTPA (<0.24 MBq/μg; $<3.6\times10^4$ MBq/μmole), only one in 50 molecules was radiolabeled. Thus, a high proportion of HER2 were bound by non-radiolabeled immunoconjugates, limiting the cytotoxic potency.

One strategy for increasing the SA of radioimmunoconjugates that we are exploring is to conjugate them to a long-chain polymer that presents multiple copies of DTPA for complexing ^{111}In [metal-chelating polymer (MCP)]. For example, biotinylated polylysine modified with up to 20 DTPA was previously suggested to increase the delivery of ^{111}In to tumors pre-targeted with streptavidin (SAv)-conjugated antibodies (5). However, the optimal MCP composition, and particularly the effect of MCP conjugation on biodistribution of the radioimmunoconjugates is not known. In this study, we synthesized a panel of three novel structurally diverse biotinylated MCPs (Fig. 1). Bi-PAm$(DTPA)_{40}$ is a polymer with a polyacrylamide backbone harboring an average of 40 pendant DTPA groups. Bi-PAsp$(DTPA)_{33}$ contains a polyaspartamide backbone, and Bi-PGlu$(DTPA)_{28}$ contains a polyglutamide backbone, harboring on average 33 and 28 DTPA groups, respectively. The synthesis and characterization of the polyacrylamide and polypeptide MCPs are reported elsewhere (6,7). With DTPA metal binding site saturation Bi-PAm$(DTPA)_{40}$ carries a net negative charge per repeat unit, whereas Bi-PAsp$(DTPA)_{33}$ and Bi-PGlu$(DTPA)_{28}$ contain zwitterionic pendant chains that carry a net neutral charge. In order to permit the study of these MCPs, and a larger library of MCPs to be synthesized in the future, the polymers were terminally modified with biotin (Bi) for facile but strong ($K_a=10^{14}\ M^{-1}$) non-covalent complexation to streptavidin (SAv) modified trastuzumab Fab fragments (SAv-Fab). This method of MCP conjugation and labeling with ^{111}In was used only to examine the effects of the backbone composition and net charge of these MCPs on tumor and normal tissue distribution in mice by comparing these properties for ^{111}In-labeled Bi-MCPs, Bi-MCP-SAv-Fab, DTPA-Fab and DTPA-SAv-Fab. Ultimately, we intend to covalently link the MCPs with the most desirable tissue distribution properties to trastuzumab IgG using site-directed chemistry that exploits the reaction of a hydrazine terminally functionalized polymer to periodate oxidized carbohydrates in the Fc-domain. These MCP-trastuzumab immunoconjugates will then be labeled to high SA with ^{111}In for enhanced Auger electron radioimmunotherapy of HER2-positive breast cancer.

MATERIALS AND METHODS

Materials

Trastuzumab was obtained from Hoffman-La Roche (Mississauga, ON, Canada). Chloroform, DTPA, $InCl_3$ (>99% purity), L-cysteine HCl monohydrate, and SAv) were obtained from Sigma-Aldrich (St. Louis, MO, USA). Immobilized papain, succinimidyl-[(*N*-maleimidopropionamido)(1)-24-ethyleneglycol] ester (SM-PEG_{24}-NHS), and 2-iminothiolane (Traut's reagent) were purchased from Pierce (Rockford, IL, USA). Chelex-100 resin, 4–20% Tris-HCl gradient mini-gel, and Coomassie brilliant blue R-250 were purchased from Bio-Rad (Mississauga, ON, Canada). PD-10 desalting columns were obtained from GE Healthcare Life Sciences (Baie d'Urfé, QC, Canada). Amicon Ultra centrifugal filter units

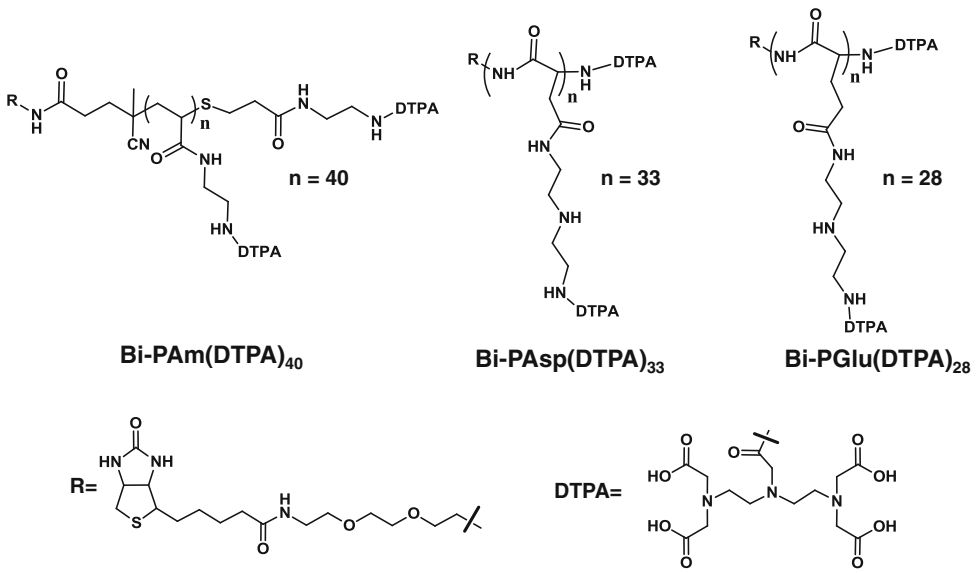

Fig. 1 Chemical structures of metal-chelating polymers (MCPs) with a terminal biotin functionality. Bi-PAm(DTPA)$_{40}$ has a polyacrylamide backbone harboring 40 pendant DTPA groups. Bi-Pasp(DTPA)$_{33}$ has a polyaspartamide backbone harboring 33 DTPA groups. Bi-PGlu(DTPA)$_{28}$ has a polyglutamide backbone harboring 28 DTPA groups. R represents biotin and the structure of DTPA is shown.

with nominal M_r cut-offs of 30, 50, and 100 kDa were purchased from Millipore (Billerica, MA, USA). $^{111}InCl_3$ (>7.4 GBq/mL) was obtained from MDS-Nordion (Kanata, ON, Canada). HER2 positive SKOV-3 human ovarian cancer cells ($1–2\times10^6$ receptors/cell) (8) were obtained from ATCC (Manassas, VA, USA). All buffers were treated with Chelex-100 resin (Biorad) to remove cationic trace metals.

Biotinylated Metal-Chelating Polymers

Details of the synthesis and characterization of the biotin-end-capped polyacrylamide MCP are described elsewhere (6). Briefly, the monomer N-{2-[(BOC) aminoethyl]} acrylamide was polymerized in the presence of a biotin RAFT agent (9,10). The number average degree of polymerization (DP_n) was characterized by ^1H NMR spectroscopy. Following removal of the Boc groups with trifluoroacetic acid, DTPA groups were attached to the primary amines of the pendant groups in a two-step reaction. First, an 80-fold excess, based on polymer $–NH_2$ groups, of DTPA in the presence of sodium hydroxide at pH 8.5 was pretreated with a limiting amount of the coupling agent 4-(4,6-dimethoxy-1,3,5-triazin-2-yl)-4-methylmorpholinium chloride (DMTMM). This solution was mixed with an aqueous solution of the polymer. By ^1H NMR, the DTPA attachment step was quantitative. Details of the synthesis and characterization of the biotin-end-capped polyaspartamide and polyglutamide MCPs were previously reported (7). Briefly, biotin-poly(β-benzyl aspartate) and biotin-poly(γ-benzyl glutamate) were prepared by ring-opening polymerization of the respective N-carboxyanhydrides initiated with (+)-biotinyl-3, 6-dioxaoctanediamine. Following aminolysis of the ester groups with diethylenetriamine, the primary amines on the pendant groups were converted to DTPA monoamides *via* coupling with DMTMM. The polymer was washed with deionized water using a spin filter (M_r cut-off=3 kDa), and then freeze dried. The characteristics of the polymers employed in these studies are shown in Table I.

Streptavidin (SAv)-Trastuzumab Fab

Fab fragments were generated by proteolysis of trastuzumab IgG using immobilized papain, then purified and derivatized with DTPA dianhydride as previously reported (11). DTPA substitution was determined by radiolabeling an aliquot of the reaction mixture with ^{111}In and analyzing the proportion of ^{111}In-DTPA-Fab and ^{111}In-DTPA by instant thin layer-silica gel chromatography (ITLC-SG), then multiplying by the mole excess of DTPA in the reaction (10:1) (12). DTPA-Fab was buffer-exchanged into phosphate buffered saline (PBS; pH 8.2) and concentrated to 2.5 mg/mL, then reacted with a 10-fold mole excess of SM-PEG_{24}-NHS for 1 h at room temperature (RT) to introduce maleimide groups for reaction with thiolated SAv (Fig. 2). SAv (5 mg/mL in PBS, pH 8.0) was thiolated by reaction with a 10-fold mole excess of 2-iminothiolane (Traut's reagent) for 1 h at RT. Both maleimide-DTPA-Fab and thiolated SAv were purified from excess reagents and buffer-exchanged into PBS (pH 7.4) by ultrafiltration on an Amicon Ultra device (M_r cut-off=30 kDa). Purified maleimide-DTPA-Fab was reacted at a 4-fold mole excess to thiolated SAv for 2 h at RT to favor monosubstitution by SAv. Finally, SAv-Fab was purified from excess SAv by ultrafiltration on an Amicon Ultra device (M_r cut-off=100 kDa).

Characterization of SAv-Trastuzumab Fab

Trastuzumab Fab purity was assessed by SDS-PAGE under reducing (dithiothreitol) and non-reducing conditions on a

Table I Properties of Metal-Chelating Polymers (MCPs)

MCP	DP_n [a]	PDI [b]	Na^+ ions per DTPA [c]	Water molecules per DTPA [c]	Adjusted molecular weight [d]
Bi-PAm$(DTPA)_{40}$	40	1.2	2.8	2.1	25 kDa
Bi-PAsp$(DTPA)_{33}$	33	1.13	2.6	2.7	23 kDa
Bi-PGlu$(DTPA)_{28}$	28	1.16	2.3	1.6	19 kDa

[a] Determined by ^{1}H NMR of the polymer produced in the initial polymerization reaction

[b] PDI=M_w/M_n as determined for the metal-free polymer by aqueous SEC using poly(methacrylic acid) standards

[c] The mass loss as determined by isothermal thermogravimetric analysis at 100°C is due to loss of water from the sample. The subsequent mass loss in isothermal TGA at 600°C is due to conversion of the residual material to Na_2CO_3 (14)

[d] Calculated from the degree of polymerization and includes the Na^+ ions and water molecules determined by TGA

4–20% Tris-HCl gradient mini-gel stained with Coomassie brilliant blue R-250. Fab and SAv-Fab were also analyzed by size-exclusion (SE)-HPLC on a BioSep SEC-S4000 column (300×4.6 mm; Phenomenex, Torrance, CA, USA) eluted with 100 mM NaH_2PO_4 buffer (pH 7.0) at a flow rate of 0.35 mL/min using a Series 200 pump (PerkinElmer, Wellesly, MA, USA) interfaced with a diode array detector (PerkinElmer) set at 280 nm. Protein standards [carbonic anhydrase (29 kDa), albumin (66 kDa), amylase (200 kDa), and blue dextran (2000 kDa); Sigma-Aldrich] were used to construct a calibration curve to estimate the M_r of SAv-Fab. Protein concentration was measured on a UV-visible spectrophotometer (Ultrospec 3100 pro, GE Healthcare Life Sciences) at 280 nm by applying a blended extinction coefficient for SAv-Fab (2.34 $cm^{-1}(mg/mL^{)-1}$) based on the average extinction coefficients for SAv and Fab [3.20 $cm^{-1}(mg/mL)^{-1}$ and 1.49 $cm^{-1}(mg/mL)^{-1}$], respectively], assuming monosubstitution of trastuzumab Fab with SAv based on the SE-HPLC analysis and the reaction ratio used (4:1 for Fab: SAv).

Complexation of Bi-MCPs to SAv or SAv-Trastuzumab Fab

Approximately 10 µg of Bi-MCPs were complexed to 40 µg of SAv-Fab, or to 10 µg SAv (total volume 15 µL), by incubation for 30 mins at RT. The mole ratio of SAv-Fab to Bi-MCP was 1:1. The resulting complexes were buffer-exchanged into 100 mM sodium acetate (pH 6.0) by ultrafiltration on an Amicon Ultra device (M_r cut-off=50 kDa).

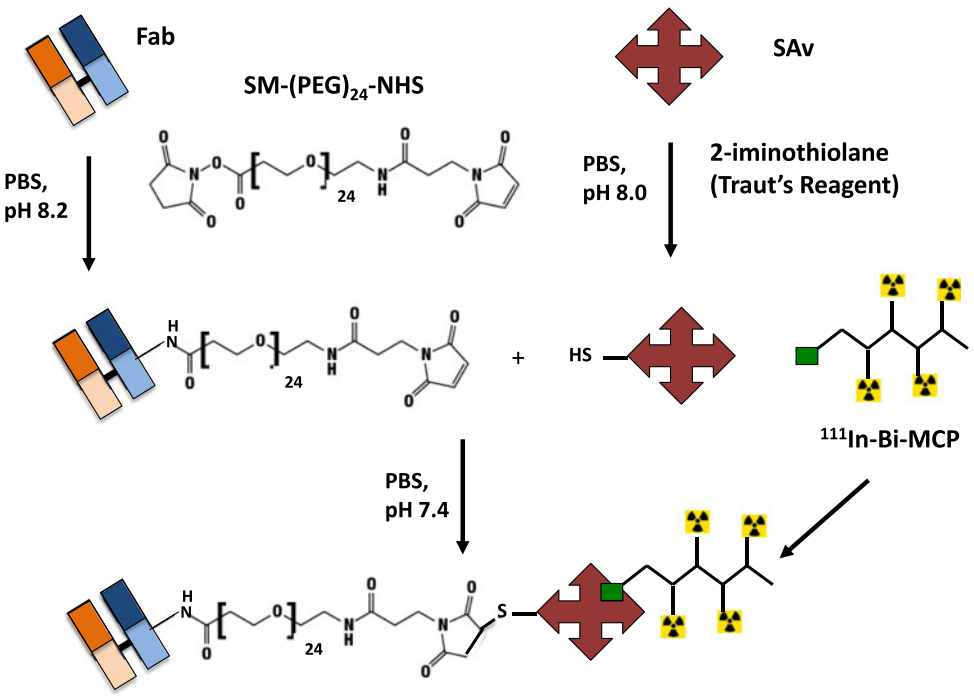

Fig. 2 Conjugation scheme for linking SAv to trastuzumab Fab and subsequent complexation with MCPs containing a biotin end-group and radiolabeled with ^{111}In.

Radiolabeling with ^{111}In

Bi-MCPs, SAv-Fab (modified with DTPA), Bi-MCP-SAv-Fab complexes, and DTPA-Fab were radiolabeled by incubation of 10 μg in 100 mM sodium acetate (pH 6.0) with $^{111}InCl_3$ at 0.04 MBq/μg for biodistribution studies or with 3.7 MBq/μg for imaging studies for 1 h at RT. In some cases, DTPA groups on Bi-MCPs were saturated with stable indium following ^{111}In-labeling, by incubation with a 50-fold mole excess of $InCl_3$ relative to total DTPA in 100 mM sodium acetate (pH 6.0) for 1 h at RT. Excess $InCl_3$ was removed by ultrafiltration on an Amicon Ultra device (M_r cut-off=30 kDa). The radiochemical purity was measured by ITLC-SG in 100 mM sodium citrate (pH 5.0). The R_f values of ^{111}In-labeled complexes and free ^{111}In were 0.0 and 1.0, respectively. To determine if incubation of the radioimmunoconjugates with stable indium displaced ^{111}In, 0.1 nmoles of uncomplexed Bi-MCPs were radiolabeled with 4 MBq of ^{111}In, then exposed to a 50-fold mole excess of $InCl_3$ for up to 72 h at RT. The radiochemical purity of the ^{111}In-MCPs was measured by ITLC-SG immediately after radiolabeling and then every 24 h. The maximum achievable SA was studied by labeling decreasing amounts of the Bi-MCPs (2, 0.2, 0.02 or 0.002 μg) or DTPA-Fab (10, 1.0, 0.1, and 0.01 μg) with a constant amount of $^{111}InCl_3$ (3.7 MBq) in 100 mM sodium acetate (pH 6.0) for 1 h and measuring the percent labeling efficiency (LE) by ITLC-SG. The minimum quantity providing a LE of >70% was taken as the maximum SA practically achievable, since this LE facilitated purification to a final purity >90%.

HER2 Immunoreactivity

The HER2 binding of trastuzumab-Fab SAv-Fab labeled directly with ^{111}In after DTPA derivatization or SAv-Fab complexed to Bi-MCPs for labeling with ^{111}In was determined by incubating HER2-positive SKOV-3 human ovarian cancer cells, grown overnight in wells in 24-well plates at 1.5×10^5 cells per well, with 10 nM of the radioimmunoconjugates (0.5–1 MBq/μg) in 0.5 mL of serum-free medium for 3 h at 4°C. In addition the HER2 binding of ^{111}In-labeled Bi-MCPs was determined. Non-specific binding was estimated by repeating the assay in the presence of a 100-fold molar excess of trastuzumab IgG. The medium was removed and the adherent cells were rinsed with PBS (pH 7.4), then solubilized in 100 mM NaOH at 37°C for 30 mins. The dissolved cells were transferred to γ-counting tubes and the total cell-bound radioactivity was measured in a γ-counter. Specific binding was calculated by subtracting non-specific binding from total binding. The effect of saturation of DTPA on the Bi-MCPs complexed to SAv-Fab was determined by repeating the assay following incubation of the radioimmunoconjugates with a 50-fold excess of stable $InCl_3$ relative to the number of DTPA groups. Specific HER2 binding was calculated as the percent of total cell bound ^{111}In.

Tissue Biodistribution and Imaging Studies

The biodistribution of ^{111}In-labeled Bi-MCPs alone or complexed to SAv, and trastuzumab Fab, or SAv-Fab derivatized with DTPA was determined in non tumor-bearing female Balb/c mice. Groups of 3–5 mice were injected intravenously (tail vein) with 0.2–0.4 MBq (10 μg) of Bi-MCPs or the radioimmunoconjugates and sacrificed at 24 h post-injection. Samples of blood and selected normal tissues were collected, weighed and transferred to γ-counting tubes. Tissue radioactivity was measured in a γ-counter and expressed as percent injected dose/g (% ID/g). In addition, the total percent recovery of radioactivity from the collected tissues was calculated by multiplying the % ID/g values by standard organ weights measured previously for Balb/c mice in our laboratory (13). MicroSPECT/CT imaging was performed up to 72 h post-injection in Balb/c mice injected intravenously with 20–37 MBq (10 μg) of ^{111}In-labeled DTPA-Fab, SAv-Fab, Bi-MCP-SAv or Bi-MCP-SAv-Fab. Mice were anesthetized by inhalation of 2% isofluorane in O_2. Imaging was performed on a NanoSPECT/CT tomograph (Bioscan) equipped with four NaI detectors and fitted with 1.4-mm multi-pinhole collimators (full width at half maximum≤1.2 mm). A total of 24 projections were acquired in a 256×256 acquisition matrix with a minimum of 80,000 counts per projection. Image reconstruction was performed using InVivoScope software (Ver 1.34beta6; Bioscan) with an ordered-subset expectation maximization algorithm (9 iterations). Cone-beam CT images were acquired (180 projections, 1 s/projection, 45 kVp) before microSPECT images. Co-registration of microSPECT and CT images was performed using InvivoScope software.

Tumor and Normal Tissue Localization

The tumor and normal tissue localization of ^{111}In-labeled Bi-PAsp(DTPA)$_{33}$ or Bi-PGlu(DTPA)$_{28}$ complexed to SAv-Fab was determined in female CD1 athymic mice (Charles River, Boston, MA) with subcutaneous, HER2-overexpressing SKOV-3 xenografts. Groups of 3–4 mice with SKOV-3 tumors (8 mm in diameter) were injected intravenously with 0.2–0.4 MBq (10 μg) of ^{111}In-Bi-PAsp(DTPA)$_{33}$-SAv-Fab or ^{111}In-Bi-PGlu(DTPA)$_{28}$-SAv-Fab with DTPA groups saturated with stable $InCl_3$ or with these radioimmunoconjugates at 3 h after pre-injection with a 100-fold excess of unlabeled trastuzumab IgG (1 mg) to block tumor HER2 receptors. The mice were sacrificed at 48 h post-injection then tumor and normal tissue uptake was measured by γ-scintillation counting and expressed as %

ID/g. All animal studies adhered to the "Principles of Laboratory Animal Care" (NIH publication #85-23, revised in 1985) and were conducted under a protocol (No. 282.9) approved by the Animal Care Committee at the University Health Network following Canadian Council on Animal Care (CCAC) guidelines.

Statistical Analysis

Data are presented as mean ± SEM. Statistical analyses were performed with an unpaired *t*-test or analysis of variance (one way ANOVA) using Prism Ver 4.0 software (GraphPad Software Inc., San Diego, CA). $p<0.05$ was considered significant.

RESULTS

Metal Chelating Polymers

The structures of Bi-PAm$(DTPA)_{40}$, Bi-PAsp$(DTPA)_{33}$ and PGlu$(DTPA)_{28}$ polymers are shown in Fig. 1. The subscripts refer to the number average degree of polymerization and the polydispersities were relatively narrow. The freeze-dried polymer samples were partially neutralized to the corresponding sodium salt. To convert mass of polymer to moles of polymer molecules, we determined the "effective" molecular weight which included both the number of Na^+ ions per repeat unit and the mean number of water molecules per repeat unit remaining in the polymer sample. These values were determined by thermogravimetric analysis, as previously described (14). Each polymer contained between 2 and 3 Na^+ ions per DTPA group. The characteristics of the polymers are shown in Table I. The molecular weight adjusted for the number of Na^+ ions and water molecules per DTPA was 25, 23 and 19 kDa, respectively, for Bi-PAm$(DTPA)_{40}$, Bi-PAsp$(DTPA)_{33}$ and PGlu $(DTPA)_{28}$.

Streptavidin (SAv)-Trastuzumab Fab

Fab fragments were obtained in high purity (>95%) by proteolysis of trastuzumab IgG using immobilized papain (Fig. 3a). Fab fragments were modified with 2.1 ± 0.1 DTPA groups per molecule by reaction with a 10-fold mole excess of DTPA dianhydride. SAv-trastuzumab Fab was synthesized by reaction of maleimide-derivatized DTPA-Fab with thiolated SAv (Fig. 2). SE-HPLC of SAv-trastuzumab Fab (Fig. 3b and c) showed one broad major peak with retention time (t_R) of 9.3 mins with a shoulder at t_R=10.1 mins. By reference to a calibration curve of the logarithm of M_r *vs.* V_e/V_0 [*i.e.* elution volume (V_e) divided by the void volume (V_0) of the column), the t_R of the major peak corresponded to a protein with M_r=130 kDa. This molecular size was slightly greater than expected for one trastuzumab-Fab (M_r=50 kDa) conjugated to one SAv molecule (M_r= 60 kDa). The broader SAv-Fab peak compared to the narrower peak for DTPA-Fab (t_R=10.4 mins; Fig. 3b) or SAv (t_R=10.3 mins; Fig. 3c) suggests that a proportion of the immunoconjugates may be composed of more than one Fab linked to SAv, since these were reacted at a 4:1 mole ratio.

Radiolabeling with ^{111}In

SAv-trastuzumab Fab was complexed to Bi-PAm$(DTPA)_{40}$, Bi-PAsp$(DTPA)_{33}$ or Bi-PGlu$(DTPA)_{28}$ and labeled with ^{111}In. Alternatively, DTPA-Fab was labeled directly with ^{111}In, or conjugated to SAv then radiolabeled. The radiochemical purity of all radioimmunoconjugates at a SA of 0.04–37.7 MBq/μg was >95%. The radiochemical purity of ^{111}In-labeled Bi-MCPs was >95%. Incubation of ^{111}In-Bi-MCPs with a 50-fold mole excess of stable $InCl_3$ to saturate DTPA groups did not cause a major loss of ^{111}In (radiochemical purity 87–90% at 72 h). By decreasing the mass of DTPA-SAv-Fab labeled with 3.7 MBq of ^{111}In from 10 μg to 0.01 μg, we compared the SA for labeling DTPA with that for the Bi-MCPs. For practical purposes, the minimum mass that provided a LE ≥70% was used to calculate the maximum SA achievable. The maximum SA for ^{111}In-DTPA-SAv-trastuzumab Fab was 3.5×10^4 MBq/μmole. In comparison, the maximum SA for Bi-PAm$(DTPA)_{40}$, Bi-PAsp$(DTPA)_{33}$ and Bi-PGlu$(DTPA)_{28}$ labeled with ^{111}In were 3.4×10^6, 3.3×10^6, and 3.7×10^6 MBq/μmole, respectively (Table II). This represents a 100-fold increase in SA for labeling the Bi-MCPs with ^{111}In compared to DTPA-Fab-SAv.

HER2 Immunoreactivity

DTPA-trastuzumab Fab or SAv-Fab labeled with ^{111}In bound specifically to HER2-positive SKOV-3 cells (Fig. 4). There was no difference in the proportions of radioactivity displaced by trastuzumab IgG for ^{111}In-DTPA-Fab and ^{111}In-DTPA-SAv-Fab and these values were >90–95% ($p>0.05$; Fig. 4a). The proportion of total binding displaced by trastuzumab IgG for SAv-Fab complexed to Bi-PAm$(DTPA)_{40}$, Bi-PAsp$(DTPA)_{33}$ or Bi-PGlu$(DTPA)_{28}$ was 40–45% ($p>0.05$; Fig. 4b). Saturation of DTPA groups with stable $InCl_3$ to decrease the negative charges on the MCPs did not increase the specific cell binding ($p>0.05$; Fig. 4b). The specific binding of uncomplexed ^{111}In-labeled Bi-MCPs to SKOV-3 cells was <3–5% ($p>0.05$; Fig. 4c).

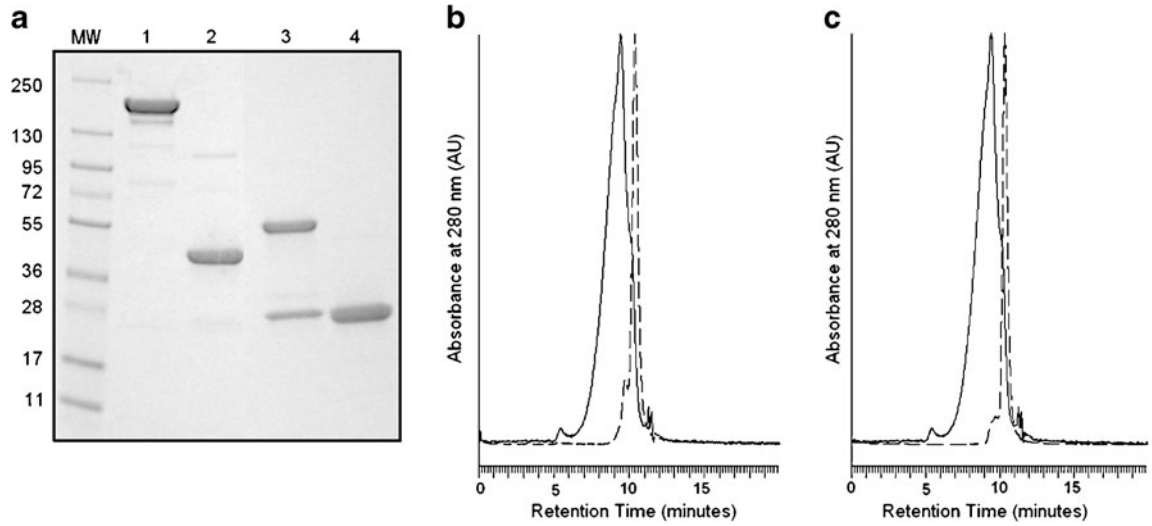

Fig. 3 (**a**) SDS-PAGE analysis of trastuzumab IgG and Fab fragments on a 4–20% Tris-HCl gradient gel stained with Coomassie Brilliant Blue under non-reducing and reducing conditions. Lanes: MW: Broad range molecular weight markers; 1: trastuzumab IgG (non-reduced); 2: trastuzumab Fab (non-reduced); 3: trastuzumab IgG (reduced); 4: trastuzumab Fab (reduced). (**b**) SE-HPLC analysis on a BioSep S-4000 column (300 × 4.6 mm ID) eluted with 0.1 M NaH_2PO_4, buffer (pH 7.0) at a flow rate of 0.35 mL/min of streptavidin (SAv)-trastuzumab Fab fragments (*solid line*) and DTPA-trastuzumab Fab (*broken line*) with UV detection at 280 nm. (**c**) SE-HPLC analysis of (SAv)-trastuzumab Fab fragments (*solid line*) and SAv (*broken line*).

Tissue Biodistribution and Imaging Studies

The highest tissue uptake of uncomplexed MCPs (Fig. 5a) at 24 h p.i. was found in the kidneys but was slightly lower for Bi-PGlu(DTPA)$_{28}$ (p=0.04) than Bi-PAm(DTPA)$_{40}$ and Bi-PAsp(DTPA)$_{33}$. There were major differences in the liver accumulation of Bi-MCPs with the highest uptake noted for Bi-PAm(DTPA)$_{40}$, which was 15-fold and 88-fold greater than for Bi-PAsp(DTPA)$_{33}$ and Bi-PGlu(DTPA)$_{28}$, respectively (p< 0.001). The blood concentrations of all uncomplexed Bi-MCPs were very low (<0.2% ID/g). When complexed to SAv, the highest liver uptake at 24 h p.i. was again found for SAv-Bi-PAm(DTPA)$_{40}$ (Fig. 5b) and was 4-fold and 15-fold greater, respectively than for SAv-Bi-PAsp(DTPA)$_{33}$ and SAv-Bi-PGlu(DTPA$_{28}$ (p<0.001). SAv complexation diminished the kidney uptake of Bi-PAm(DTPA)$_{40}$ and Bi-PAsp(DTPA)$_{33}$ by 6-fold and 2-fold, (p<0.05 and p<0.001, respectively). No significant difference in kidney accumulation was found for Bi-PGlu(DTPA)$_{28}$ with or without complexation to SAv (p>0.05). The lowest kidney uptake was noted for SAv-Bi-PAm(DTPA)$_{40}$, which was 3–5 fold less than for SAv-Bi-PAsp(DTPA)$_{33}$ and SAv-Bi-PGlu(DTPA)$_{28}$ (p<0.001).

Higher concentrations of radioactivity were found at 24 h p.i. in the blood and normal tissues except the kidneys (which exhibited lower uptake) when trastuzumab Fab was complexed to SAv (p<0.05; Fig. 6). The biodistribution of ^{111}In-labeled Bi-MCP-SAv-Fab with or without saturation by stable $InCl_3$ to decrease the negative charges on uncomplexed DTPA groups at 24 h post-injection in Balb/c mice is shown in Fig. 7. Without $InCl_3$ saturation (Fig. 7a), circulating radioactivity in the blood was 4-fold (p<0.01) and 2-fold (p<0.05) greater, respectively for ^{111}In-labeled Bi-PAsp(DTPA)$_{33}$-SAv-Fab than for Bi-PAm(DTPA)$_{40}$ or Bi-PGlu(DTPA)$_{28}$ complexed to SAv-Fab. With $InCl_3$ saturation (Fig. 7b), circulating radioactivity was increased for all complexes, and ^{111}In-labeled Bi-PAsp(DTPA)$_{33}$-SAv-Fab exhibited 3-fold higher

Table II Maximum Specific Activity (SA) Achievable for Labeling with ^{111}In

Polymer or Chelator	Mass (μg)	DTPA (μmoles × 10^{-3})	LE (%) [a]	SA (MBq/μmole × 10^3)
DTPA-SAv-Fab[b]	10	0.182	84.4	34.5
Bi-PAm(DTPA)$_{40}$	0.017	0.032	70.4	3,370
Bi-PAsp(DTPA)$_{33}$	0.017	0.026	70.0	3,310
Bi-PGLu(DTPA)$_{28}$	0.0187	0.021	76.5	3,780

Maximum SA achievable was defined as the SA for the smallest mass of polymer or chelator that provided a labeling efficiency >70%

[a] Labeling efficiency was determined by ITLC-SG after incubation with ^{111} $InCl_3$ for 1 h at RT as described in the Materials and Methods

[b] DTPA was conjugated to streptavidin-trastuzumab Fab fragments (2.1 ± 0.1 DTPA per Fab)

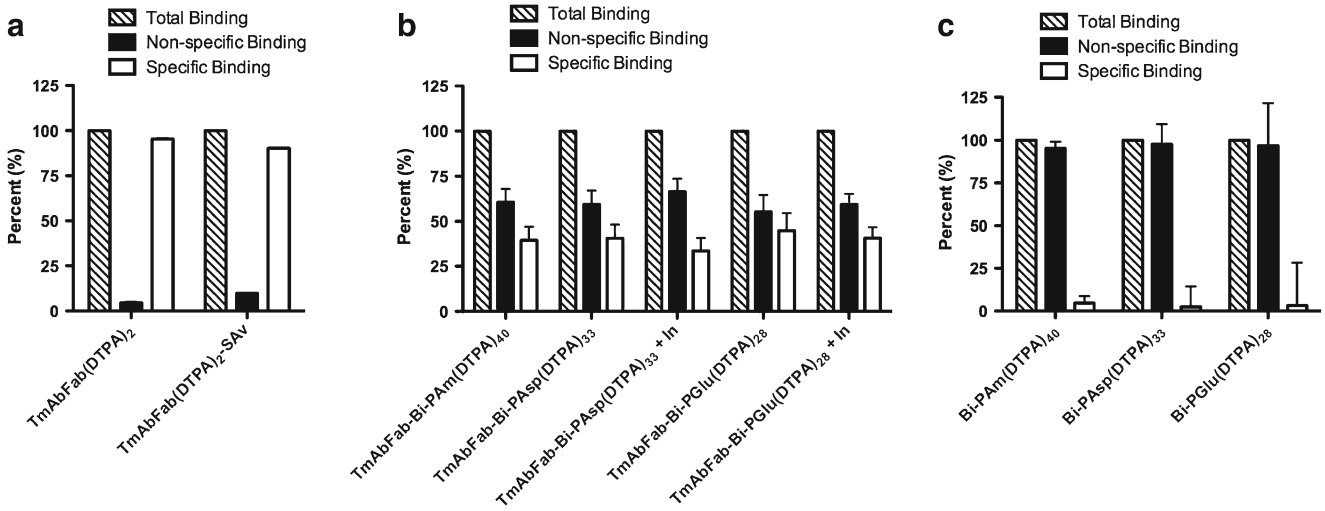

Fig. 4 **a**. Percent binding to HER2-positive SKOV-3 human ovarian cancer cells of (**a**) ^{111}In-labeled trastuzumab Fab fragments modified with DTPA [TmAbFab(DTPA)$_2$] and streptavidin-conjugated trastuzumab Fab (TmAbFab(DTPA)$_2$-SAv) or (**b**) SAv-trastuzumab Fab complexed to biotin-functionalized metal-chelating polymers [MCPs: Bi-PAm(DTPA)$_{40}$, Bi-PAsp(DTPA)$_{33}$ or Bi-PGlu(DTPA)$_{28}$] or (**c**) uncomplexed Bi-MCPs. Cells were incubated with the radioimmunoconjugates or Bi-MCPs for 3 h at 4°C in the presence (specific binding) or absence (total binding) of an excess of trastuzumab IgG as described in the Materials and Methods. Total binding was normalized to 100% and specific binding was calculated by subtracting non-specific binding from total binding. Values shown are the mean ± SEM percent binding (n=3–4).

blood concentration than Bi-PAm(DTPA)$_{40}$ or Bi-PGlu (DTPA)$_{28}$ complexed to SAv-Fab ($p<0.001$). The highest liver uptake was again found for ^{111}In-labeled Bi-PAm(DTPA)$_{40}$-SAv-Fab (Fig. 7a) but this decreased 1.5-fold by saturation of uncomplexed DTPA with stable $InCl_3$ (Fig. 7b; $p<0.05$). Liver uptake of ^{111}In-labeled Bi-PAsp(DTPA)$_{33}$ and Bi-PGlu (DTPA)$_{28}$ complexed to SAv-Fab was decreased 1.6-fold and 1.4-fold, respectively with indium saturation ($p<0.05$). Similarly, kidney uptake of Bi-PAm(DTPA)$_{33}$-SAv-Fab and Bi-PGlu(DTPA)$_{28}$-SAv-Fab was decreased 2-fold and 3-fold, respectively with indium saturation ($p<0.001$). However, indium saturation had no significant effect on the kidney uptake of ^{111}In-labeled Bi-PAsp(DTPA)$_{40}$ complexed to SAv-Fab. Spleen radioactivity was 2.7-fold and 6.4-fold higher, respectively for Bi-PAm(DTPA)$_{40}$ complexed to SAv-Fab than Bi-PAsp(DTPA)$_{33}$-SAv-Fab or Bi-PGlu (DTPA)$_{28}$-SAv-Fab ($p<0.001$). No change in spleen uptake was found with indium saturation for Bi-PGlu(DTPA)$_{28}$ or Bi-PAsp(DTPA)$_{33}$ complexed to SAv-Fab but the spleen uptake of Bi-PAm(DTPA)$_{40}$-SAv-Fab decreased 1.8-fold ($p<0.001$). There were differences in percent recovery between Bi-MCPs (Table III). The highest percent recovery was found for Bi-

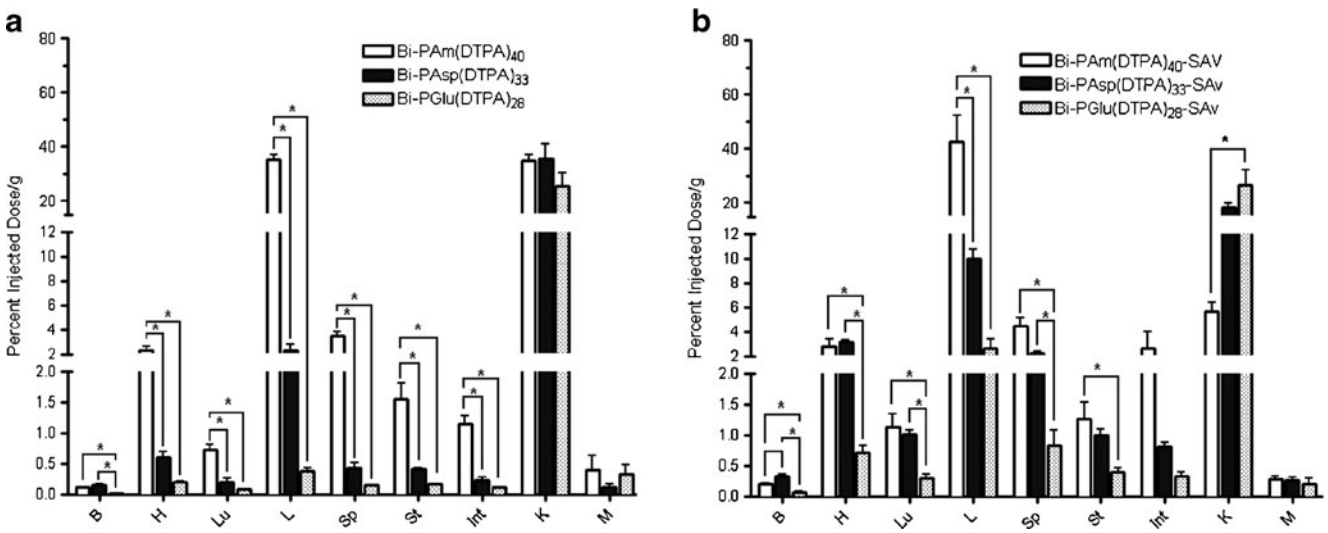

Fig. 5 Comparison of the biodistribution of ^{111}In-labeled biotinylated metal chelating polymers (Bi-MCPs) alone (**a**) or complexed to streptavidin (SAv) (**b**) at 24 h post-injection in Balb/c mice. Significant differences ($p<0.05$) between the different Bi-MCPs uncomplexed or complexed to SAv are indicated by *asterisks*. Values shown are the mean ± SEM % ID/g (n=3–5).

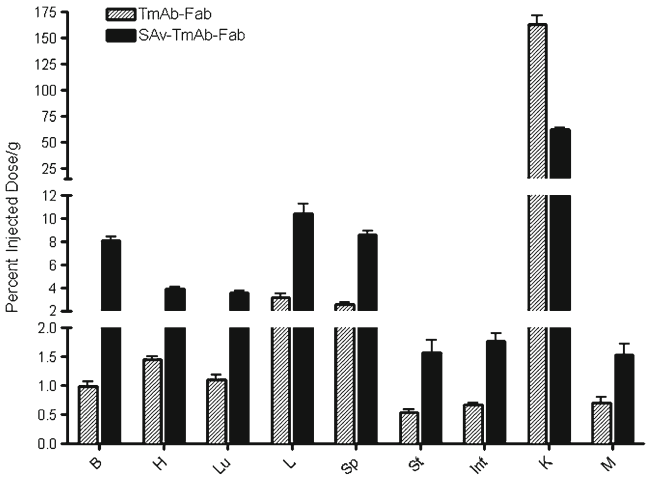

Fig. 6 Comparison of the biodistribution of ^{111}In-labeled streptavidin (SAv)-conjugated trastuzumab (TmAb) Fab and TmAb Fab fragments at 24 h post-injection in Balb/c mice. All differences in organ uptake were significant ($p < 0.05$). Values shown are the mean ± SEM % ID/g (n=3–5).

PAm(DTPA)$_{40}$ complexed to SAv-Fab which was 2-fold higher than Bi-PAsp(DTPA)$_{33}$ and 4-fold higher than Bi-PGlu(DTPA)$_{28}$. The percent recovery for Bi-PAm(DTPA)$_{40}$-SAv-Fab was 1.4-fold lower when saturated with stable indium than without indium saturation (p=0.016).

MicroSPECT/CT images at 24 h post-injection in Balb/c mice (Fig. 8) agreed with the *ex vivo* biodistribution studies. ^{111}In-trastuzumab Fab exhibited high kidney uptake with negligible levels of blood pool radioactivity (Fig. 8Aa]. SAv-Fab similarly showed high kidney uptake but also liver accumulation and circulating blood pool (Fig. 8Ab). SAv-Fab complexed to Bi-PAm(DTPA)$_{40}$ demonstrated the greatest liver uptake, low kidney accumulation and negligible levels of circulating radioactivity (Fig. 8Ac). SAv-Fab complexed to Bi-PAsp(DTPA)$_{33}$ (Fig. 8Ad) showed lower liver uptake and higher kidney uptake than when complexed to Bi-PAm(DTPA)$_{40}$. Bi-PGlu(DTPA)$_{28}$ complexed to SAv-Fab showed lower liver uptake compared to Bi-PAm(DTPA)$_{40}$ complexed to SAv-Fab, low circulating radioactivity and low kidney uptake (Fig. 8Ae). In addition, the changes in normal tissue distribution of SAv-Fab complexed to ^{111}In-labeled Bi-PGlu(DTPA)$_{28}$ were examined over a 72 h period (Fig. 8B). There appeared to be a decrease in liver and kidney accumulation at 72 h post-injection, but no major changes in normal tissue distribution were observed between 24 and 48 h post-injection.

Tumor and Normal Tissue Localization

The tumor and normal tissue distribution of ^{111}In-labeled Bi-PAsp(DTPA)$_{33}$ or Bi-PGlu(DTPA)$_{28}$ complexed to SAv-Fab with indium saturation of uncomplexed DTPA in

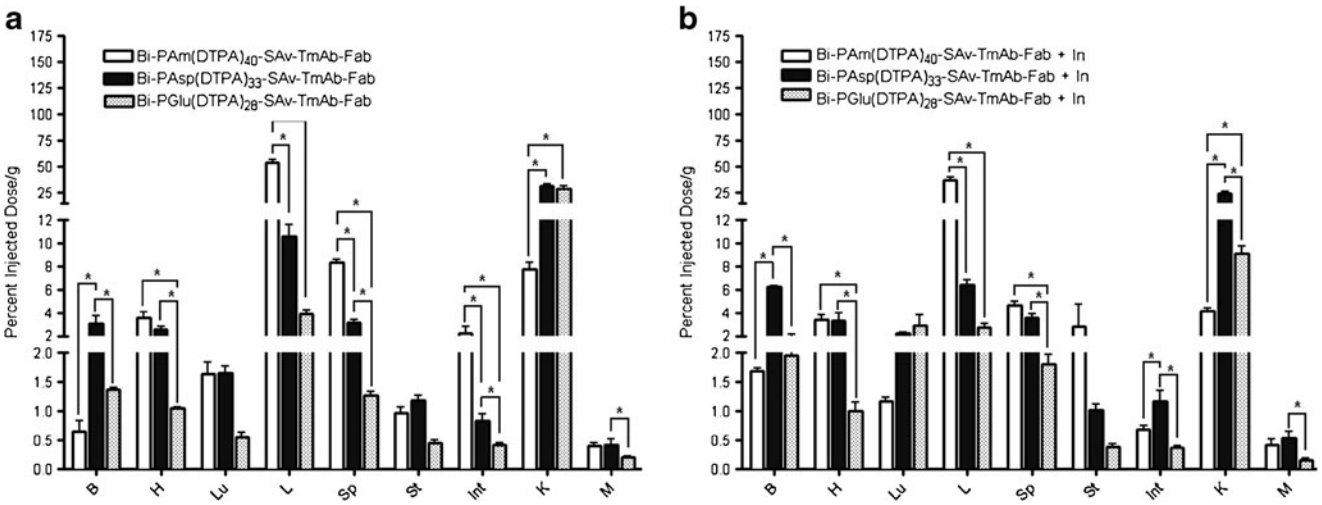

Fig. 7 Comparison of the biodistribution of ^{111}In-labeled biotinylated metal chelating polymers (Bi-MCPs) complexed to streptavidin (SAv)-conjugated trastuzumab (TmAb) Fab fragments without saturation of DTPA groups with stable indium (**a**) or with indium saturation (**b**) at 24 h post-injection in Balb/c mice. Significant differences ($p < 0.05$) between the different MCPs complexed to SAv-Fab with or without indium saturation are indicated by asterisks. Values shown are the mean ± SEM % ID/g (n=3–5).

Table III Percent Recovery of Radioactivity from Sampled Tissues in Balb/c Mice

Polymer	Uncomplexed MCPs [a]	MCP-SAv	MCP-SAv-Trastuzumab Fab	MCP-SAv-Trastuzumab Fab plus indium saturation
Bi-PAm$(DTPA)_{40}$	68.6 ± 2.5	104.3 ± 15.3	91.4 ± 4.1 [b]	64.4 ± 5.4 [c]
Bi-PAsp$(DTPA)_{33}$	18.0 ± 2.6	26.2 ± 1.5	40.6 ± 3.1 [d]	43.3 ± 1.7
Bi-PGlu$(DTPA)_{28}$	10.6 ± 1.9	12.7 ± 2.3	22.5 ± 1.5 [e]	15.6 ± 0.8

Mean ± SEM (n=3–4) recovery was calculated by multiplying the % ID/g values (Figs. 5 and 7) by standard organ weights for Balb/c mice (13)

[a] MCPs: Metal-chelating polymers; SAv: Streptavidin

[b-c] Significantly different (p=0.016)

[b-d] Significantly different (p=0.001)

[d-e] Significantly different (p=0.006)

athymic mice with subcutaneous HER2-overexpressing SKOV-3 ovarian cancer xenografts at 48 h p.i. is shown in Fig. 9. Tumor uptake of ^{111}In-Bi-PAsp$(DTPA)_{33}$-SAv-Fab was 7.0 ± 0.5% ID/g but decreased to 3.1 ± 0.7% ID/g (p< 0.05) with pre-injection of a 100-fold mole excess of trastuzumab IgG, demonstrating HER2-specific accumulation. Blood concentrations of radioactivity were 1.6 ± 0.1% ID/g without trastuzumab IgG blocking, yielding a tumor:blood ratio of >4:1. Blood radioactivity remained unchanged with excess trastuzumab IgG (1.6 ± 0.7% ID/g), resulting in a decrease in the tumor:blood ratio to <2:1. Liver and spleen uptake were reduced by trastuzumab IgG from 5.4 ± 0.4% ID/g to 3.1 ± 0.7% ID/g (p<0.05) and from 3.0 ± 0.2% ID/g to 2.4 ± 0.1% ID/g (p<0.05). In contrast, the localization of ^{111}In-Bi-PGlu$(DTPA)_{28}$-SAv-Fab in SKOV-3 tumors and in the blood and normal tissues was much lower than ^{111}In-Bi-PAsp$(DTPA)_{33}$-SAv-Fab (Fig. 9b). This was consistent with the lower percent recovery (Table III). The tumor:blood ratio for ^{111}In-Bi-PGlu$(DTPA)_{28}$-SAv-Fab was >3:1 and tumor uptake was decreased 1.5-fold by blocking with excess trastuzumab IgG, but this difference did not reach statistical significance (p=0.058).

DISCUSSION

SAv-conjugated trastuzumab Fab fragments were complexed to Bi-MCPs with different backbone composition and overall net charge, and the effects of the MCPs on the tumor and normal tissue biodistribution were studied in mice. The SAv-biotin system provided a rapid and facile method of complexing (K_a=10^{14} M^{-1}) structurally diverse MCPs to trastuzumab Fab fragments to study these properties but this strategy was intended only as a screening approach in mice, since SAv is known to be immunogenic in humans (15). Ultimately, we plan to link MCPs with the most desirable tissue distribution properties site-specifically to trastuzumab IgG by reaction of a terminally introduced hydrazine functionality with periodate-oxidized carbohydrates in the F_c-domain (16). Bi-PAm$(DTPA)_{40}$ was

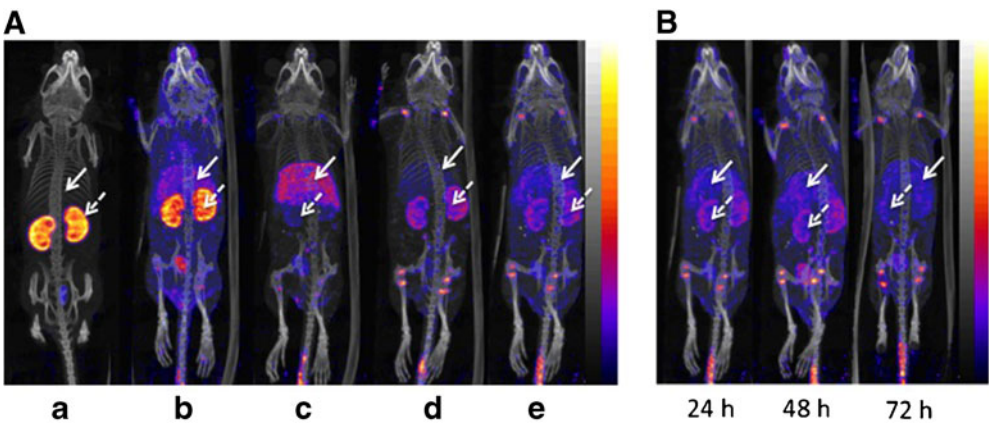

Fig. 8 (**A**) Maximum intensity projection whole body posterior microSPECT/CT images at 24 h post-injection of (**a**) ^{111}In-labeled trastuzumab Fab, (**b**) streptavidin (SAv)-trastuzumab Fab, (**c**) Bi-PAm$(DTPA)_{40}$-SAv-trastuzumab Fab, (**d**) Bi-PAsp$(DTPA)_{33}$-SAv-trastuzumab Fab, and (**e**) Bi-PGlu$(DTPA)_{28}$-SAv-trastuzumab Fab. Images were adjusted to approximately equal intensity. The position of the liver and kidneys are shown by the *solid* and *broken arrows*, respectively. (**B**) MicroSPECT/CT images of Balb/c mice at 24, 48 or 72 h post-injecction of ^{111}In-labeled Bi-PGlu$(DTPA)_{28}$-streptavidin (SAv)-trastuzumab Fab. Images were adjusted to approximately equal intensity.

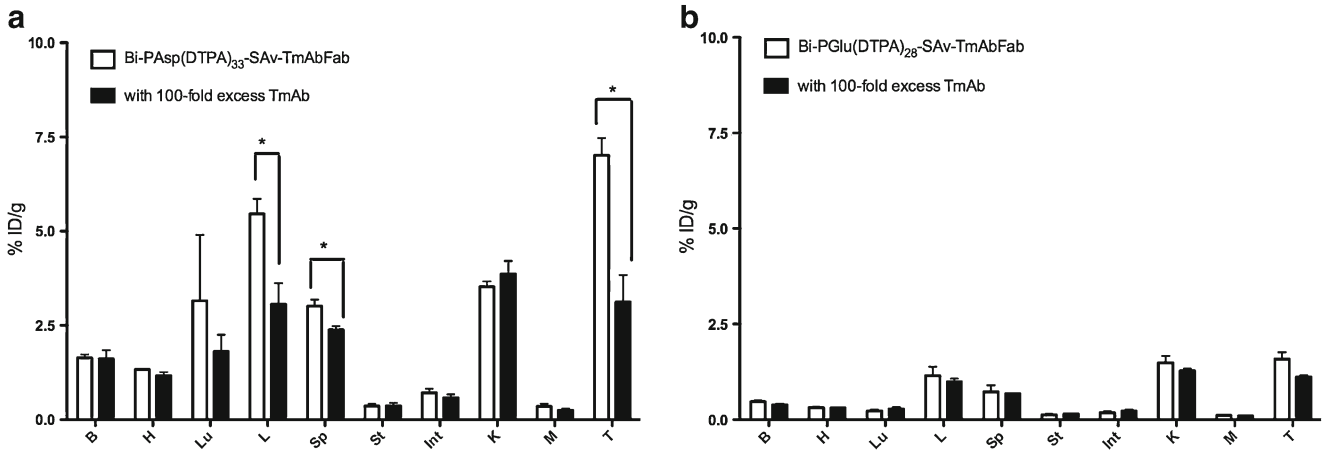

Fig. 9 Tumor and normal tissue distribution of ^{111}In-labeled (**a**) Bi-PAsp(DTPA)$_{33}$ or (**b**) Bi-PGlu(DTPA)$_{28}$ linked to SAv-trastuzumab Fab (SAv-TmAb Fab) at 48 h post-injection in athymic mice bearing subcutaneous SKOV-3 human ovarian cancer xenografts. Significant differences caused by pre-injection of a 100-fold excess of unlabeled trastuzumab 3 h prior to the radioimmunoconjugates are indicated by asterisks. Values shown are the mean ± SEM % ID/g (n=3).

composed of a polyacrylamide backbone modified with an average of 40 pendant DTPA groups for complexing ^{111}In and had a polydispersity (M_w/M_n) of 1.2 (Table I). Based on the known pK_a values of DTPA monoamide of 1.8, 3.8, 6.4, and 9.9 (17), it was expected that each metal-free DTPA unit would carry 2 to 3 negative charges at pH 7.5, whereas each DTPA monoamide carrying an In^{3+} ion would have a net charge of (−1). Bi-PAsp(DTPA)$_{33}$ and Bi-PGlu(DTPA)$_{28}$ were composed of polyaspartamide or polyglutamide backbones with an average of 33 or 28 pendant DTPA groups, respectively, and contained zwitterionic pendant chains that yielded a net neutral charge when bound to indium. These polymers had a polydispersity of 1.13 and 1.16, respectively.

Conjugation of thiolated SAv to maleimide-derivatized trastuzumab Fab did not decrease specific binding to HER2-positive SKOV-3 cells (Fig. 4). Hainsworth *et al.* similarly found preserved HER2 immunoreactivity for trastuzumab conjugated to SAv using the complementary chemistry involving reaction of maleimide-modified SAv and reduced thiols on trastuzumab IgG (18). Trastuzumab Fab fragments are tolerant to macromolecular modification since we recently linked these to the surface of block copolymer micelles labeled with ^{111}In and these micelles were specifically bound and internalized into HER2-positive breast cancer cells (19). However, complexing Bi-PAm(DTPA)$_{40}$, Bi-PAsp(DTPA)$_{33}$ or Bi-PGlu(DTPA)$_{28}$ to SAv-trastuzumab Fab decreased the proportion of specific binding to SKOV-3 cells compared to Fab or SAv-Fab by 2-fold (Fig. 4). There were no differences in HER2 immunoreactivity among the different polymer-SAv-Fab radioimmunoconjugates and there were no changes in HER2 binding with saturation of DTPA with stable indium which neutralizes 3 of the 4 negative charges from the DTPA carboxylic acid groups. This suggests that decreased HER2 immunoreactivity was not related to the composition or net charge of the polymers. One possible explanation could be that these polymers fold around the Fab fragments, masking the HER2 binding domain or they may perturb the tertiary structure of the Fab fragments through charge interactions. SE-HPLC analysis (Fig. 3) indicated that the Fab fragments were predominantly modified with one SAv molecule per Fab. In comparison, relatively preserved HER2 immunoreactivity has been reported for trastuzumab IgG conjugated to polyamidoamine (PAMAM) dendrimers for high SA labeling with ^{111}In (20,21). The lower proportion of total binding to SKOV-3 cells displaced by an excess of trastuzumab IgG for the Bi-MCPs complexed to SAv-Fab (40–45%) compared to uncomplexed SAv-Fab or Fab (90–95%) suggests that these polymers may impart some non-specific binding on the immunoconjugates. This was not related to the charges on the Bi-MCPs since the proportion of trastuzumab-displaced radioactivity did not change with indium saturation of uncomplexed DTPA groups on Bi-PAsp(DTPA)$_{33}$ or Bi-PGlu(DTPA)$_{28}$. Only 3–5% of the binding of ^{111}In-labeled uncomplexed MCPs was displaced by trastuzumab IgG (Fig. 4c), further suggesting that the MCPs may impart some non-specific binding characteristics.

The concentrations of radioactivity at 24 h p.i. in the blood and all normal tissues were higher for ^{111}In-labeled SAv-Fab than unmodified Fab fragments (Fig. 6). These findings can be explained by the increase in molecular size shown by the SE-HPLC analysis (Fig. 3) suggesting that one SAv molecule was linked to one Fab fragment. The resulting immunoconjugates (estimated M_r=130 kDa) would have a size that exceeds the renal threshold for filtration (M_r<60 kDa) thus slowing the elimination and increasing tissue uptake (22). Biodistribution studies (Figs. 5 and 7) and microSPECT/CT imaging (Fig. 8) showed that ^{111}In-labeled Bi-PAm(DTPA)$_{40}$ complexed to SAv or SAv-Fab was more rapidly eliminated from the blood and exhibited higher liver uptake in mice than Bi-PAsp (DTPA)$_{33}$ and Bi-PGlu(DTPA)$_{28}$ alone or complexed to SAv

or SAv-Fab. These differences may be due to the backbone composition and/or the charge of these polymers. The negative charge of Bi-PAm(DTPA)$_{40}$ may promote binding and internalization in the liver by Kupffer cells or hepatocytes, causing sequestration of radioactivity from the blood (23). Saturation of uncomplexed DTPA with stable indium decreases the negative charges of Bi-PAm(DTPA)$_{40}$ as well as those on the other Bi-MCPs and resulted in a 2-fold lower liver uptake when complexed to SAv-Fab (Fig. 7). Slinkin *et al.* conjugated F(ab′)$_2$ fragments of mAb F6 to polylysine polymers which carried either a net positive charge (Poly 1) or had increasing negative charge (Poly 2 and Poly 3) and were modified with DTPA for ^{111}In labeling (24). The slowest blood clearance was observed for ^{111}In-Poly 1-F(ab′)$_2$ while conjugation to Poly 2 and 3 polymers caused more rapid elimination from the blood, particularly for the highly negatively-charged Poly 3. Liver uptake at 24 h post-injection was not different between ^{111}In-labeled Poly 1, 2 or 3-conjugated F(ab′)$_2$, but kidney uptake was 4-fold greater and spleen uptake was 3-fold higher for Poly 1-conjugated F(ab′)$_2$. Xiao *et al.* reported that highly positively- or negatively-charged PEGylated oligocholic acid micelles exhibited greater liver uptake than neutral micelles in mice bearing SKOV-3 tumor xenografts (25). This suggests that the negative charge of the Bi-PAm(DTPA)$_{40}$ polymers was most likely responsible for the rapid blood clearance of the SAv-trastuzumab-Fab radioimmunoconjugates and their hepatic accumulation in mice. The higher percent recovery of radioactivity from the collected tissues in our study (Table III) was consistent with the greater tissue uptake and retention of Bi-PAm(DTPA)$_{40}$ than the other MCPs complexed to SAv or SAv-trastuzumab Fab. The lower percent recovery for ^{111}In-labeled Bi-PAm (DTPA)$_{40}$-SAv-trastuzumab Fab with saturation of DTPA with stable indium to reduce the negative charges on the MCPs agrees with the effect of these charges on promoting tissue sequestration.

Based on the tissue distribution and microSPECT/CT imaging results, the stable indium saturated, neutrally charged Bi-PAsp(DTPA)$_{33}$ and Bi-PGlu(DTPA)$_{28}$ polymers were chosen to examine *in vivo* tumor targeting. In athymic mice with subcutaneous SKOV-3 tumors, there was very good tumor localization (7% ID/g) of SAv-Fab complexed to ^{111}In-labeled Bi-PAsp(DTPA)$_{33}$ at 48 h post-injection (Fig. 9a). Tumor uptake was decreased 2-fold with administration of excess trastuzumab IgG, demonstrating HER2-mediated localization. In contrast, the accumulation of ^{111}In-Bi-PGlu (DTPA)$_{28}$-SAv-Fab in SKOV-3 tumors as well as in the blood and normal tissues was much lower (Fig. 9b). Although tumor uptake of ^{111}In-Bi-PAsp(DTPA)$_{33}$-SAv-Fab was decreased 1.5-fold by trastuzumab IgG blocking, this difference did not reach statistical significance (p=0.058). The reason for the lower uptake in the liver and spleen for ^{111}In-Bi-PAsp (DTPA)$_{33}$-SAv-Fab with administration of excess trastuzumab IgG is not known. The tumor uptake of ^{111}In-Bi-PAsp (DTPA)$_{33}$-SAv-Fab compared favourably to that previously reported by our group for ^{111}In-labeled trastuzumab Fab in mice with HER2-overexpressing BT-474 human breast cancer xenografts (8.4±1.8% ID/g) (11) or SKOV-3 human ovarian cancer xenografts (4.0±0.9% ID/g) (8).

When we initiated these studies, we anticipated that MCPs with a polyglutamide backbone may have advantages over those with a polyaspartamide backbone *in vivo*, based on a report from the Kataoka laboratory (26) that polyaspartamide with diethylenetriamine pendant groups (PAsp(DET)) degraded rapidly (hours) *in vitro* under model physiological conditions, whereas a corresponding PGlu(DET) polymer was stable. However, when we investigated the degradation rate of Bi-PAsp(DTPA)$_{33}$ saturated with stable indium under model physiological conditions (10 mM phosphate buffer, pH 7.4, 150 mM NaCl at 37°C) we found that the DTPA pendant group slowed the rate substantially, with negligible degradation over 24 to 48 h (7). The more rapid degradation of PAsp (DET) compared to PAsp(DTPA) is likely due to an acceleration of the backbone hydrolysis rate by the positive charge associated with each pendant group in PAsp(DET). As expected, we found that Bi-PGlu(DTPA) was stable to these conditions. The maximum SA practically achieved for radiolabeling Bi-PAm(DTPA)$_{40}$, Bi-PAsp(DTPA)$_{33}$, and Bi-PGlu (DTPA)$_{28}$, (3.4×10^6, 3.3×10^6, and 3.7×10^6 MBq/μmole, respectively) was 100-fold higher than DTPA-SAv-Fab (3.4×10^4 MBq/μmole). These results suggest that conjugation of these MCPs could substantially increase the SA of the ^{111}In-labeled radioimmunoconjugates.

CONCLUSIONS

We conclude that zwitterionic MCPs composed of a polyaspartamide backbone and harboring 33 pendant DTPA groups exhibited the most desirable tumor and normal tissue distribution properties. We are now developing conjugation chemistry to site-specifically link these MCPs to the Fc-domain of trastuzumab for high SA labeling with ^{111}In for enhanced Auger electron radioimmunotherapy of HER2-positive breast cancer.

ACKNOWLEDGMENTS AND DISCLOSURES

The authors gratefully acknowledge financial support from the Canadian Institutes of Health Research/Natural Sciences and Engineering Research Council Collaborative Health Research Program (Grant No. CPG95268). D. W. was the recipient of a Feodor-Lynen Fellowship from the Alexander von Humboldt Foundation and G. N. N. M. was the recipient of a Canadian Institutes of Health Research

Pre-Doctoral Scholarship from the Biological Therapeutics Strategic Training Program.

REFERENCES

1. McKeage K, Perry CM. Trastuzumab: a review of its use in the treatment of metastatic breast cancer overexpressing HER2. Drugs. 2002;62:209–43.
2. Costantini DL, Chan C, Cai Z, Vallis KA, Reilly RM. ^{111}In-labeled trastuzumab (Herceptin) modified with nuclear localizing sequences (NLS): an Auger electron-emitting radiotherapeutic agent for HER2/neu-amplified breast cancer. J Nucl Med. 2007;48:1357–68.
3. Costantini DL, Hu M, Reilly RM. Peptide motifs for insertion of radiolabeled biomolecules into cells and routing to the nucleus for cancer imaging or radiotherapeutic applications. Cancer Biother Radiopharm. 2008;23:3–24.
4. Costantini DL, Bateman K, McLarty K, Vallis KA, Reilly RM. Trastuzumab-resistant breast cancer cells remain sensitive to the Auger electron-emitting radiotherapeutic agent ^{111}In-NLS-trastuzumab and are radiosensitized by methotrexate. J Nucl Med. 2008;49:1498–505.
5. Torchilin VP. Biotin-conjugated polychelating agent. Bioconjug Chem. 1999;10:146–9.
6. Liu P, Boyle AJ, Lu Y, Reilly RM, Winnik M. Biotinylated polyacrylamide-based metal-chelating polymers and their influence on antigen recognition following conjugation to a trastuzumab Fab fragment. Biomacromolecules 2012. doi:10.1021/bm300843u.
7. Lu Y, Chau M, Boyle AJ, Liu P, Niehoff A, Weinrich D, *et al.* Effect of pendant group structure on the hydrolytic stability of polyaspartamide polymers under physiological conditions. Biomacromolecules. 2012;13:1296–306.
8. Chan C, Scollard DA, McLarty K, Smith S, Reilly RM. A comparison of ^{111}In- or ^{64}Cu-DOTA-trastuzumab Fab fragments for imaging subcutaneous HER2-positive tumor xenografts in athymic mice using microSPECT/CT or microPET/CT. EJNMMI Res. 2011;1:11.
9. Green M, Berman J. Preparation of pentafluorophenyl esters of FMOC protected amino acids with pentafluorophenyl trifluoroacetate. Tetrahedron Letters. 1990;31:5851–2.
10. Grayson DH, Roycroft ED. Synthesis of butanolides *via* intramolecular acylative ring-opening reactions of 3-(tetrahydro-2-furyl)propanoic acid derivatives. J Chem Soc Chem Commun. 1992;18:1296–7.
11. Tang Y, Wang J, Scollard DA, Mondal H, Holloway C, Kahn HJ, *et al.* Imaging of HER2/neu-positive BT-474 human breast cancer xenografts in athymic mice using ^{111}In-trastuzumab (Herceptin) Fab fragments. Nucl Med Biol. 2005;32:51–8.
12. Scollard DA, Chan C, Holloway CMB, Reilly RM. A kit to prepare ^{111}In-DTPA-trastuzumab (Herceptin) Fab fragments injection under GMP conditions for imaging or radioimmunoguided surgery of HER-2 positive breast cancer. Nucl Med Biol. 2011;38:129–36.
13. Reilly RM, Chen P, Wang J, Scollard D, Cameron R, Vallis KA. Preclinical pharmacokinetic, biodistribution, toxicology and dosimry studies of ^{111}In-DTPA-hEGF - an Auger electron-emitting radiotherapeutic agent for EGFR-positive breast cancer. J Nucl Med. 2006;47:1023–31.
14. Majonis D, Ornatsky O, Kinach R, Winnik MA. Curious results with palladium- and platinum-carrying polymers in mass cytometry bioassays and an unexpected application as a dead cell stain. Biomacromolecules. 2011;12:3997–4010.
15. Knox SJ, Goris ML, Tempero M, Weiden PL, Gentner L, Breitz H, *et al.* Phase II trial of yttrium-90-DOTA-biotin pretargeted by NR-LU-10 antibody/streptavidin in patients with metastatic colon cancer. Clin Cancer Res. 2000;6:406–14.
16. Rodwell JD, Alvarez VL, Lee C, Lopes AD, Goers JWF, King HD, *et al.* Site-specific covalent modification of monoclonal antibodies: *in vitro* and *in vivo* evaluation. Proc Natl Acad Sci USA. 1986;83:2632–6.
17. Sherry AD, Cacheris WP, Kuan KT. Stability constants for Gd^{3+} binding to model DTPA-conjugates and DTPA-proteins: implications for their use as magnetic resonance contrast agents. Magn Reson Med. 1988;8:180–90.
18. Hainsworth JE, Harrison P, Mather SJ. Novel preparation and characterization of a trastuzumab-streptavidin conjugate for pretargeted radionuclide therapy. Nucl Med Commun. 2006;27:461–71.
19. Hoang B, Reilly RM, Allen C. Block copolymer micelles target Auger electron radiotherapy to the nucleus of HER2-positive breast cancer cells. Biomacromolecules. 2012;13:455–65.
20. Miyano T, Wijagkanalan W, Kawakami S, Yamashita F, Hashida M. Anionic amino acid dendrimer-trastuzumab conjugates for specific internalization in HER2-positive cancer cells. Mol Pharmaceut. 2010;7:1318–27.
21. Shukla R, Thomas TP, Peters JL, Desai AM, Kukowska-Latallo J, Patri AK, *et al.* HER2 specific tumor targeting with dendrimer conjugated anti-HER2 mAb. Bioconjug Chem. 2006;17:1109–15.
22. Reilly RM, Sandhu J, Alvarez-Diez TM, Gallinger S, Kirsh J, Stern H. Problems of delivery of monoclonal antibodies. Pharmaceutical and pharmacokinetic solutions. Clin Pharmacokinet. 1995;28:126–42.
23. Caliceti P, Veronese FM. Pharmacokinetic and biodistribution properties of poly(ethylene glycol)-protein conjugates. Adv Drug Deliv Rev. 2003;55:1261–77.
24. Slinkin MA, Curtet C, Faivre-Chauvet A, Sai-Maurel C, Gestin JF, Torchilin VP, *et al.* Biodistribution of anti-CEA $F(ab')_2$ fragments conjugated with chelating polymers: influence of conjugate electron charge on tumor uptake and blood clearance. Nucl Med Biol. 1993;20:443–52.
25. Xiao K, Li Y, Luo J, Lee JS, Xiao W, Gonik AM, *et al.* The effect of surface charge on *in vivo* biodistribution of PEG-oligocholic acid based micellar nanoparticles. Biomaterials. 2011;32:3435–46.
26. Itaka K, Ishii T, Hasegawa Y, Kataoka K. Biodegradable polyamino acid-based polycations as safe and effective gene carrier minimizing cumulative toxicity. Biomaterials. 2010;31:3707–14.